



# 1 **Rainfall recharge thresholds decrease after an intense fire over a near-** 2 **surface cave at Wombeyan, Australia**

3  
4 Christina Song<sup>1</sup>, Micheline Campbell<sup>2,1</sup> and Andy Baker<sup>1,3</sup>

5  
6 <sup>1</sup>Earth and Sustainability Science Research Centre, School of Biological, Earth and Environmental Sciences, UNSW, Sydney  
7 2052, Australia

8 <sup>2</sup>Climate Geochemistry Department, Max Planck Institute for Chemistry, Mainz, Germany

9 <sup>3</sup>ANSTO, Lucas Heights, Australia

10

11 *Correspondence to:* Andy Baker (a.baker@unsw.edu.au)

12 **Abstract.** Quantifying the amount of rainfall needed to generate groundwater recharge is important for the sustainable  
13 management of groundwater resources. Here, we quantify rainfall recharge thresholds using drip loggers situated in a near-surface  
14 cave: Wildman's cave at Wombeyan, southeast Australia. In just over two years of monitoring, 42 potential recharge events were  
15 identified in the cave, approximately 4 m below land surface which comprises a 30° slope with 37% bare rock. Recharge events  
16 occurred within 48 hours of rainfall. Using daily precipitation data, the median 48 h rainfall needed to generate recharge was 19.8 mm,  
17 without clear seasonal variability. An intense experimental fire experiment was conducted 18 months into the monitoring period: the  
18 median 48 h rainfall needed to generate recharge was 22.1 mm before the fire (n=22) and 16.4 mm after the fire (n=20), with the  
19 decrease in rainfall recharge most noticeable starting three months after the fire.. Rainfall recharge thresholds and number of potential  
20 recharge events at Wildman's Cave are consistent with those published from other caves in water-limited Australia. At Wildman's  
21 Cave, we infer that soil water storage, combined with the generation of overland flow over bare limestone surfaces is the pathway for  
22 water movement to the subsurface via fractures and that these determine the rainfall recharge threshold. Immediately after the fire,  
23 surface ash deposits initially retard overland flow, and after ash removal from the land surface, soil loss and damage decrease the  
24 available soil water storage capacity, leading to more efficient infiltration and a decreased rainfall recharge threshold.

## 25 **1 Introduction**

26 Groundwater recharge is a vital process where freshwater replenishes itself to support and nurture a healthy ecosystem and  
27 provide a source of water for human use. The groundwater recharge process is strongly controlled by climatic and geologic factors  
28 in association with temporal variability (Ajami, 2022). In warmer climates, evapotranspiration of water can occur at a faster  
29 rate than it can be replenished by rainfall, limiting the occurrence of recharge to infrequent, high magnitude rainfall events (for  
30 example, Boas and Mallants, 2022). In lithologies that have low permeability, recharge is limited to preferential flow pathways  
31 such as fractures, leading to a very low fraction of annual rainfall generating recharge (Kotchoni et al., 2019).

32 Quantifying both the timing and amount of groundwater recharge is a challenge, yet fundamentally important if changes in groundwater recharge  
33 over time are to be quantified (e.g. Noori et al., 2023). At the event scale, only a few techniques are available to identify recharge, and the source



34 and age of the water being analysed is often uncertain. Recharge events can be identified in some groundwater wells or bores where fluctuations  
35 in groundwater level can be observed over time using the water table fluctuation method (Healy and Cook, 2002). Recently, a new approach  
36 has been proposed that uses loggers in underground spaces such as caves that are situated in the unsaturated zone (Baker et al., 2020, 2021). This  
37 approach identifies when water percolates into the subsurface void and has been proposed as another method for identifying both the timing of  
38 recharge events at the event scale and the amount of rainfall needed for caves, tunnels and mines (Baker et al., 2024).

39 Fire can have an impact on subsurface hydrology, however its role in recharge processes is less well understood. For example,  
40 ash beds have a variable impact on hydrology and have been shown both to increase runoff and reduce infiltration (e.g. Gabet  
41 and Sternberg, 2008) and store water, increasing infiltration (e.g. Woods and Balfour, 2008), and in general ash has a higher  
42 carrying capacity than soil. However, the formation of ash crusts may enhance overland flow and impede infiltration (Balfour  
43 e al., 2014; Onda, 2008). Ash crusts are thought to form due to physical-chemical properties of ash as well as rainfall  
44 compaction. Ashes which contain oxides (well-combusted ashes) may form ash crusts due to the hydration and recrystallisation  
45 of carbonate crusts (Balfour et al., 2014; Bodí et al., 2014). These crusts are generally ephemeral, but post-fire changes to  
46 hydrology may persist for several years (Cerdá, 1998). Furthermore, ash can clog soil pores, further reducing infiltration  
47 capacity (Bodí et al., 2014; Woods and Balfour, 2008).

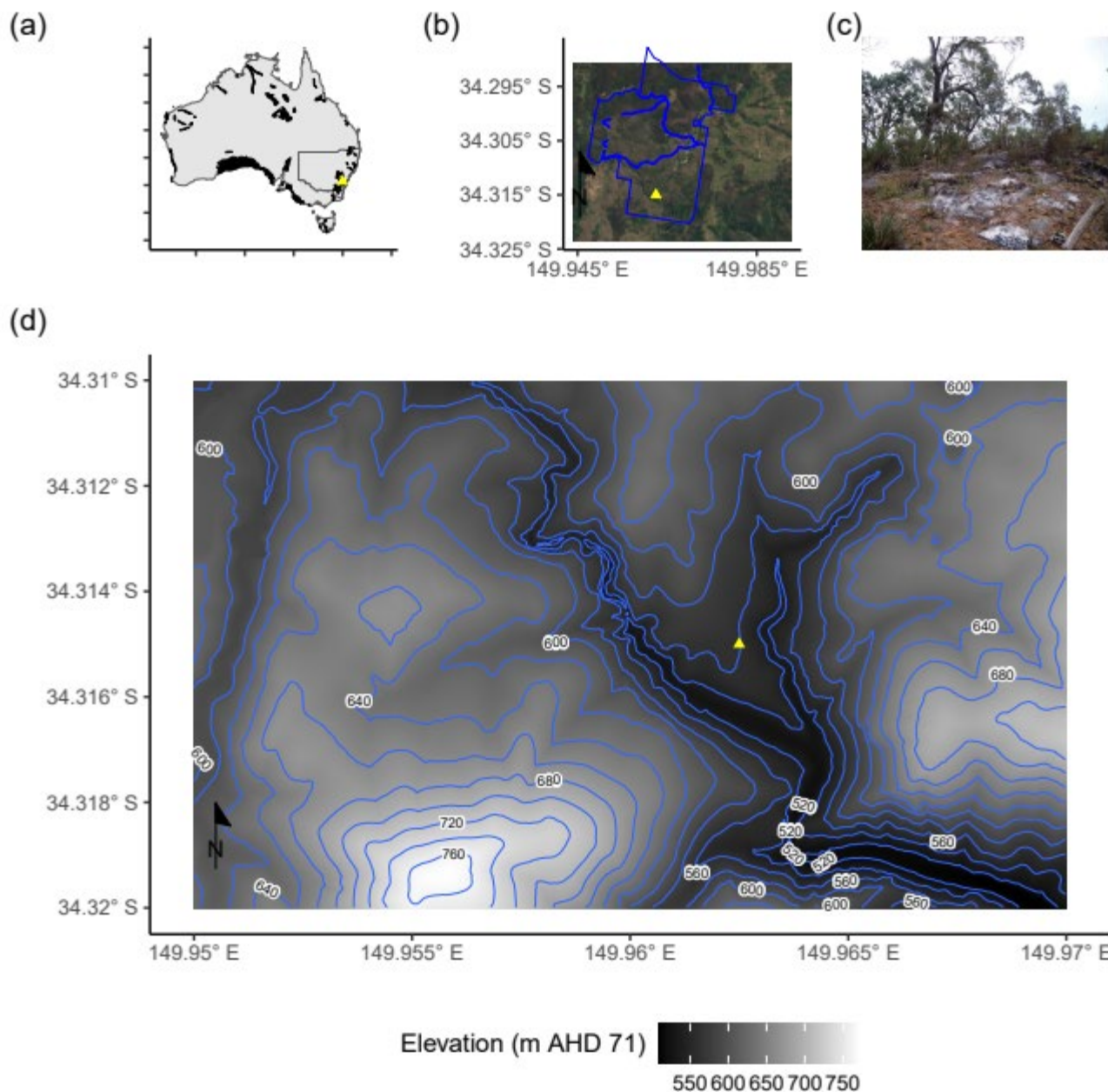
48 Here, we use the unsaturated zone monitoring approach that uses loggers in underground spaces to investigate the potential  
49 impacts of fire on the amount of rainfall needed to generate recharge. Between December 2014 and May 2017, before and  
50 after a fire, cave drip water hydrological monitoring was undertaken at a shallow cave site in southeast Australia as part of a  
51 wider investigation of the impacts of fire on karst processes. The experimental design was to have at least one year of  
52 monitoring data before and after a fire, to assess potential impacts on the cave environment. Hydrograph analysis and  
53 percolation water geochemical analyses from that study were published by Bian et al., 2019, however, the amount of rainfall  
54 needed to generate recharge using cave percolation waters was not determined. Bian et al. 2019 demonstrated percolation  
55 water events into the cave were characterized by hydrographs of shorter duration and with higher maxima after the fire.  
56 Combined with inorganic geochemical and water isotope data, this observation was interpreted as increased preferential  
57 (fracture) flow and decreased diffuse flow (from the soil) after the fire. Because Bian et al., 2019, did not analyse the hydrology  
58 data to obtain rainfall recharge thresholds for each potential recharge event, this analysis is undertaken here, to (1) quantify  
59 the rainfall recharge threshold for the site (2) to investigate seasonal variations in rainfall recharge threshold and the possible  
60 impact of surface fire on rainfall recharge thresholds and (3) compare results to those reported from sites in southern and  
61 eastern Australia (Baker et al., 2020, 2021).

## 62 **2 Site Description and Methods**

63 Wildman's Cave is located at 608 m above sea level in the Wombeyan Caves Karst Conservation Reserve (34° 19" S, 149°  
64 58" E), in the south-eastern part of New South Wales, Australia (Fig. 1). It is formed in the Silurian age Wombeyan Limestone  
65 formation, a marble which is highly fractured with no matrix porosity remaining (Osborne, 1993). Subsurface water movement  
66 is therefore dominated by fracture and conduit flows. The cave is small and shallow with a narrow pothole type entrance and  
67 a total of 42 m of cave passage containing numerous stalactites (Wylie and Wylie, 2004). The whole cave is less than 4 m  
68 depth below land surface. The surface above the cave comprises a 30° sloping ridgeline. 37% of the surface has no soil cover,



69 the remaining land surface has a median 5 cm soil cover, reaching a maximum 33 cm where soil has accumulated in fractures.  
70 Vegetation, where present, comprises dry sclerophyll shrubs and grasses.



71

72 **Figure 1.** a) Australia with karst overlay, yellow triangle indicates the study site (WOKAM; from Chen et al (2017)). B) Sentinel S2 visible  
73 image, with bounds of the Wombeyan Karst Reserve. SentinelS2 True Colour image [2024]. Retrieved from Copernicus Dataspace [7  
74 December 2024], processed by Copernicus. Wombeyan boundary: State Government of NSW and NSW Department of Climate Change,  
75 Energy, the Environment and Water 2000, NSW National Parks and Wildlife Service (NPWS) Estate, accessed from The Sharing and  
76 Enabling Environmental Data Portal [<https://datasets.secd.nsw.gov.au/dataset/9bad468a-c2a6-4c90-bfaa-8ac8af72e925>], date accessed

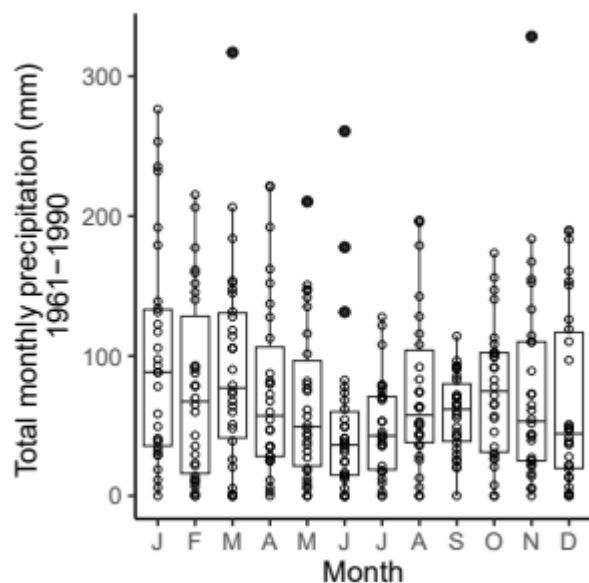


77 2024-11-07. c). Photograph of the surface above the cave one day after the fire (source: Andy Baker) d) Digital elevation model. Yellow  
78 triangle is the approximate position of the cave. DEM from NSW Government, DFSI Spatial Services 2 km x 2 km 2 metre Resolution  
79 Digital Elevation Model. Accessed via Elvis - Elevation and Depth - Foundation Spatial Data 19/12/2024

80

81 Annual precipitation at the site over the last ten years has a long-term average of 802 mm, annual areal potential  
82 evapotranspiration (PET) is 1228 mm, and modelled actual evapotranspiration (AET) is 680 mm (data from the Australian  
83 Water Landscape Model (AWRA-L) v7, Frost and Shokri, 2021). Temperature at Taralga (17 km distant and 845 m above sea  
84 level) ranges from an average minimum of 6.1 °C to an average maximum of 18.3 °C. Over the study period, precipitation at  
85 the site was close to the long-term average (2015 annual precipitation: 773 mm; 2016 annual precipitation: 843 mm) and areal  
86 PET slightly higher than the long-term average (2015 annual areal PET: 1307 mm; 2016 annual areal PET: 1331 mm). There  
87 is minor seasonality in precipitation, with monthly precipitation in the cooler months (June and July) tending to be both lower  
88 and less variable than during the warmer months (Fig. 2). We note, however, that even the cool months can report very high  
89 monthly totals, likely owing to the impact of East Coast Lows, intense low pressure systems that form off the east coast of  
90 Australia, and which are most common in autumn and winter (Pepler et al., 2014).

91



92 **Figure 2.** Total monthly precipitation, 1961-1991.

93

94 We used data from eleven Stalagmate © drip loggers that were deployed throughout the cave between December 2014 and  
95 January 2017 and for which hydrograph analysis has been previously presented in Bian et al., 2019. Only four loggers remained  
96 in operation from January 2017 to May 2017: data from this period was not analysed quantitatively. Monitoring ceased in  
97 May 2017, one year after an experimental fire occurred on the surface above the cave.. Loggers were programmed to record  
98 the total number of drips in a 15-minute period. Recharge events were identified here through visual inspection of the time  
99 series and cross-checked with the events identified in Bian et al., (2019) and a date allocated. To determine the amount of

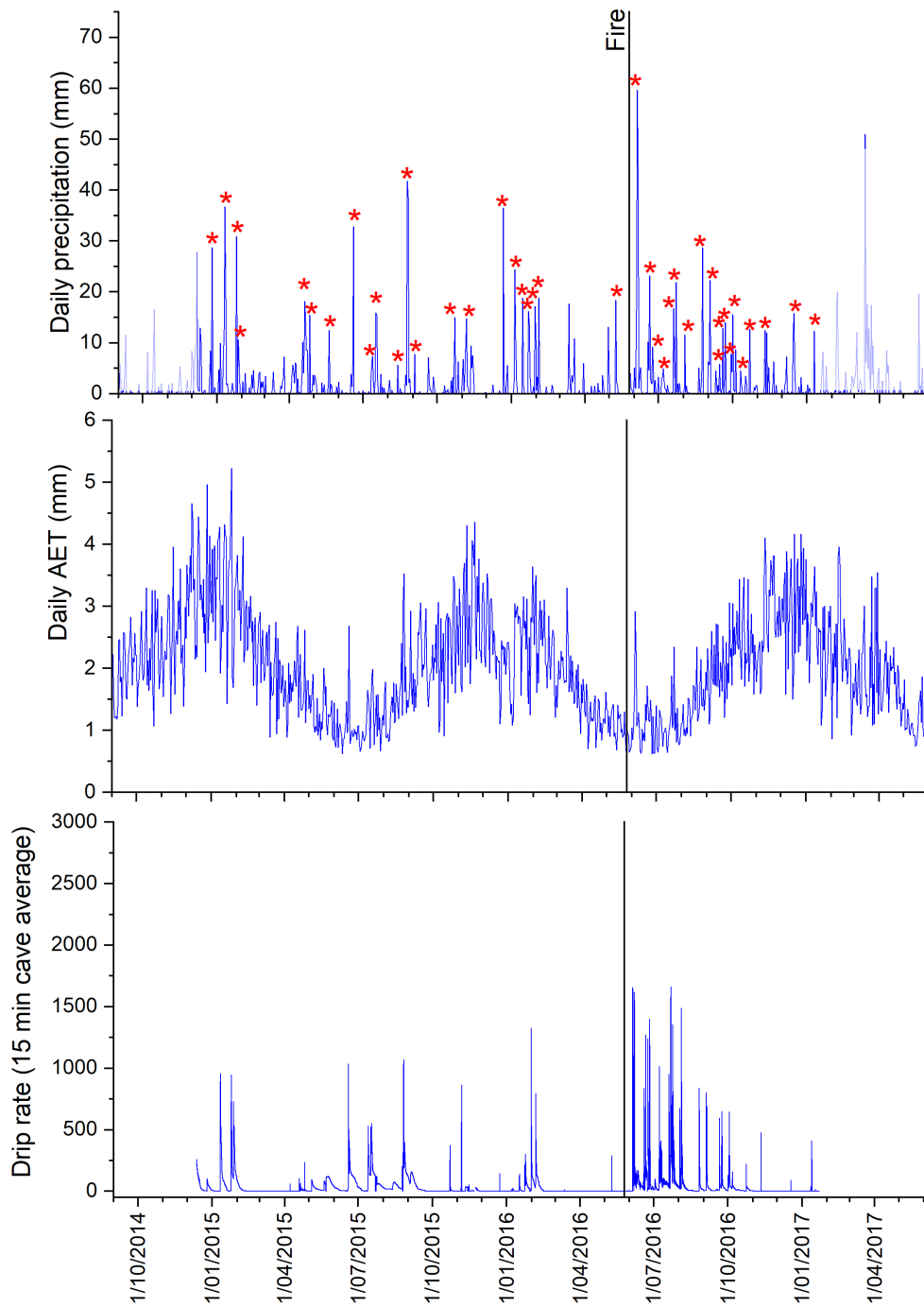


100 rainfall needed to generate recharge, daily rainfall records were obtained for the six days up to and including the date of  
101 recharge. Since daily rainfall amounts are collected for the 24 hours up to 9 am, this analysis also considered precipitation on  
102 the day after recharge was observed to ensure that all contributing rainfall was included. Precipitation data was taken from the  
103 Bureau of Meteorology station at Wombeyan Caves (station number 63093) as well as gridded daily precipitation from the  
104 AWRA-L, accessed via the Australian Water Outlook website (Bureau of Meteorology, 2024). Where there were incomplete  
105 returns from the Bureau of Meteorology station, the AWRA-L gridded daily precipitation value was used.

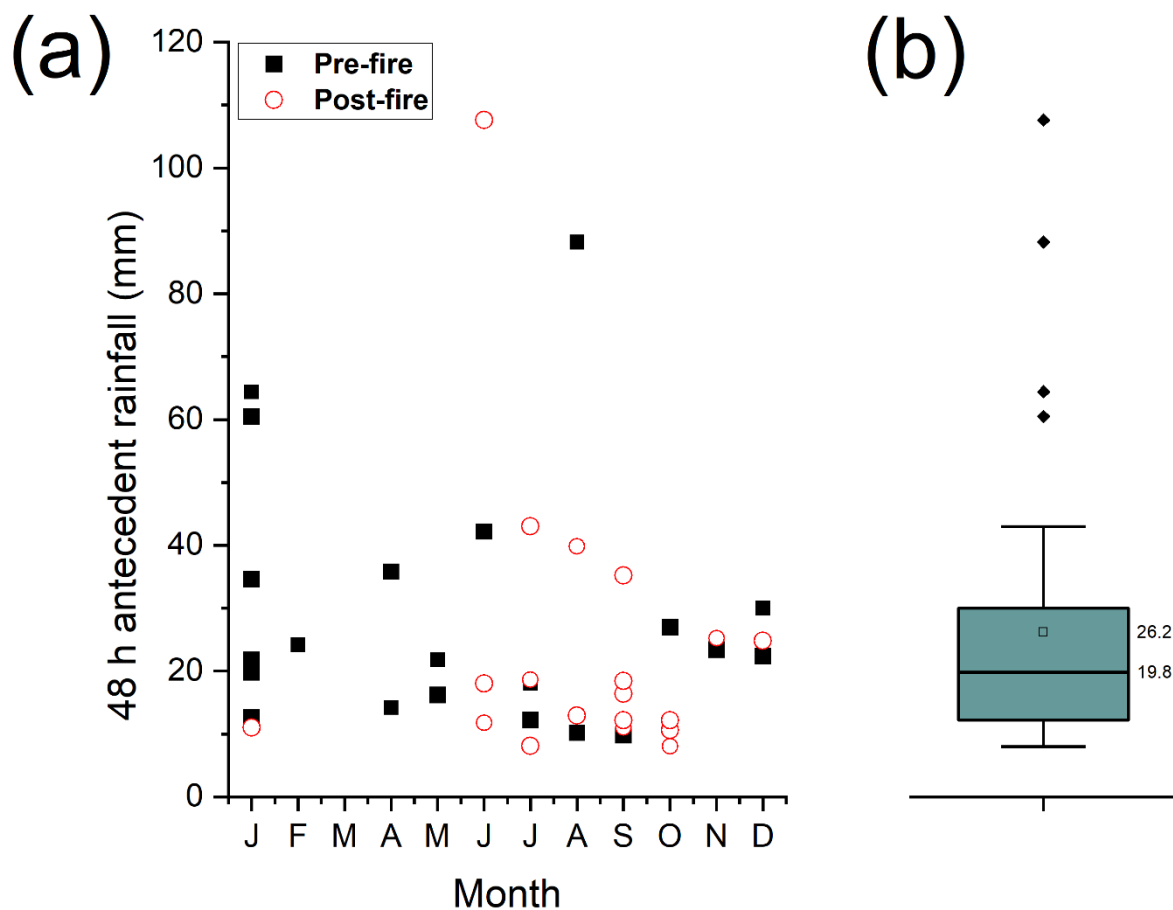
106 An intense experimental fire over the cave (10 m x 10 m) occurred on 25<sup>th</sup> May 2016, which resulted in the surface litter being  
107 generally consumed by the fire, with ash accumulations of several centimetres depth occurring in places. Thermocouples  
108 placed at 12 cm depth in the soil recorded maximum temperatures between 30 and 930 °C, with spalling of the limestone and  
109 calcining observed in localised hotspots. Bian et al., (2019) analysed drip water hydrograph structure, water isotope  
110 composition and geochemistry before and after the fire. After the fire, recharge event hydrographs were peakier and of shorter  
111 duration than pre fire. Stable water isotope composition of drip waters was relatively constant pre-fire, with a rapid shift to a  
112 more negative oxygen isotope composition immediately post-fire, returning to the pre-fire baseline after six months. This was  
113 interpreted to be due to the complete evaporation of soil and shallow vadose zone water in the fire, with the post-fire drip water  
114 isotopic compositions reflect that of the first recharge events after the fire rather than a long-term mixed precipitation signal,  
115 and subsequent rainfall events over the next six months replenishing the water in the soil and shallow vadose zone. Water  
116 geochemical analyses demonstrated a decrease in rock-water residence time post-fire, with an associated increase in ash-  
117 derived sulphur immediately post-fire and limited evidence of other ash-derived geochemical tracers. For further details see  
118 Bian et al. (2019).

### 119 **3 Results**

120 Daily rainfall (Bureau of Meteorology) and evapotranspiration (AWRA-L), and the 15-minute total number of drips averaged  
121 for all loggers are shown in Figure 3. A total of 42 recharge events occurred between December 2014 to January 2017, an  
122 average of 1.6 recharge events per month. One observed recharge event (4<sup>th</sup> May 2015) had only 1.6 mm of associated  
123 antecedent rainfall associated with it, and we assume that this was a locally heavier event that was not captured in the gauge ~  
124 2 km away. This event is not included in subsequent rainfall recharge threshold calculations. Recharge events occurred in all  
125 months except March, and only seven recharge events were observed in the late summer / early autumn months of February  
126 to May (Fig. 4). Excluding the May 2015 event, 22 recharge events were observed before the fire and another 19 after the fire.  
127 Analysis of the daily rainfall distribution before and after the fire showed very little difference (Fig. 5), indicating that any  
128 observed differences in rainfall recharge thresholds is unlikely to be due to differences in daily precipitation.



129 **Figure 3.** Daily precipitation (light blue when outside the monitoring period) with timing of recharge events shown by red asterisks, daily  
130 AET (from the AWRA-L) and average 15 min total drips.



131 **Figure 4** a 48 h antecedent rainfall classified by month and whether before or after fire. b box and whisker plot of all 48 h rainfall amounts  
132

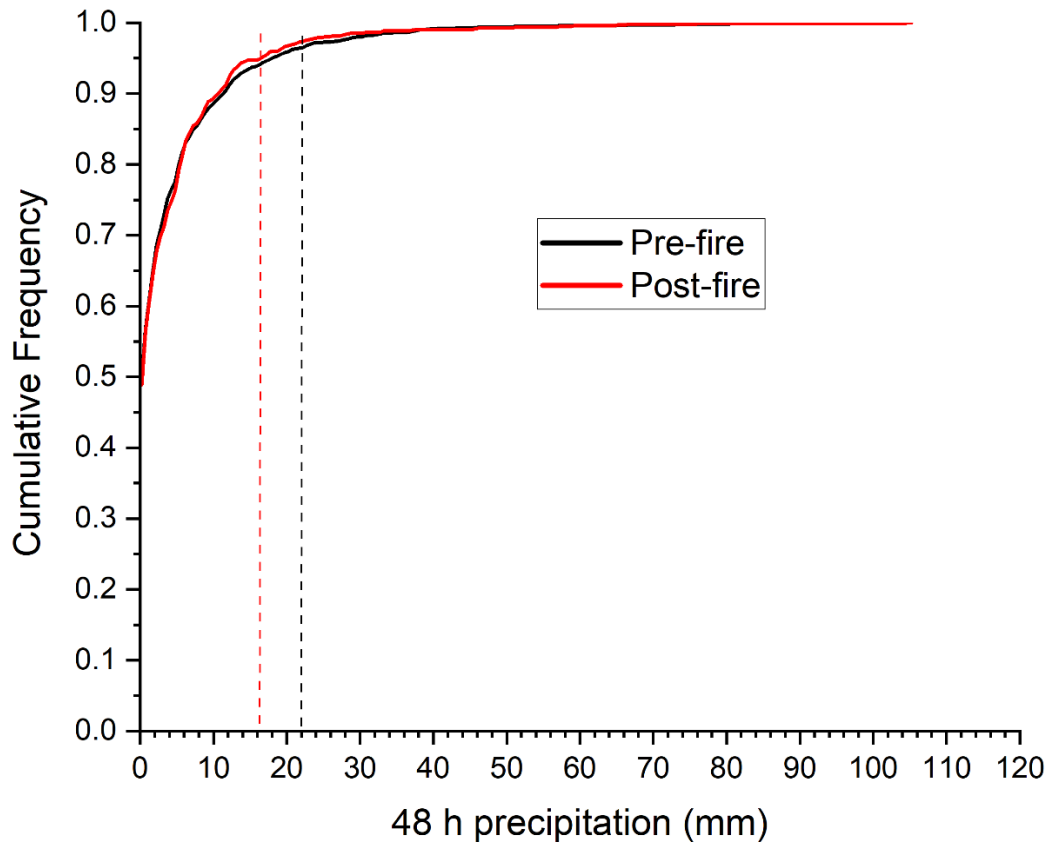
133 Five of the events occurred when there were incomplete daily precipitation returns from the Bureau of Meteorology rain gauge  
134 and for these events the gridded AWRA-L data was used. Comparison of the Bureau of Meteorology and AWRA-L 48 h  
135 rainfall totals for those events (data is presented in Table 1) suggest that AWRA-L 48 h precipitation is 28% lower than the  
136 Bureau of Meteorology gauge. No correction was applied.

137

138 Antecedent conditions were analysed for the 24, 48, 72, 96, 120 and 144 hours prior to each observed recharge event (Fig.  
139 A1). Considering all recharge events, compared to the 144 (six day) sum antecedent precipitation, 48% of all precipitation  
140 occurred in the first 24 hours and 69% of all precipitation occurred within the 48 hours prior to recharge. The relative



141 contribution to the total percentage rainfall over 72, 96 and 120 hours continued to decline, and therefore we use the 48 h  
142 antecedent total precipitation amount to determine rainfall recharge thresholds.



143  
144 **Figure 5.** Cumulative frequency of 48 h precipitation pre (black) and post (red) fire. Dashed lines show the median rainfall recharge  
145 thresholds.



Pre-fire				Post-fire			
Event	Date	48 h precipitation (mm) BoM	48 h precipitation (mm) AWRA-L	Event	Date	48 h precipitation (mm) BoM	48 h precipitation (mm) AWRA-L
1	25/12/2014	22.4	28.7	24	4/06/2016	107.6	76.1
2	11/01/2015	60.5	55.5	25	18/06/2016	11.8	14.8
3	24/01/2015	64.4	30.9	26	24/06/2016	18	13.6
4	27/01/2015	<i>19.8</i>	19.8	27	6/07/2016	<i>8.1</i>	8.1
5	20/04/2015	35.8	32.4	28	20/07/2016	18.6	23
6	25/04/2015	14.2	15.5	29	22/07/2016	43	22.2
8	19/05/2015	16.2	14.6	30	2/08/2016	<i>12.9</i>	12.9
9	18/06/2015	42.2	38.3	31	24/08/2016	39.8	33.1
10	13/07/2015	12.2	9.8	32	2/09/2016	35.2	28
11	16/07/2015	<i>18.1</i>	18.1	33	14/09/2016	11	6.3
12	12/08/2015	10.2	5.9	34	18/09/2016	16.4	13.9
13	25/08/2015	88.2	80.5	35	21/09/2016	18.4	16.6
14	3/09/2015	9.8	8	36	29/09/2016	12.2	12.1
15	22/10/2015	27	20.8	37	4/10/2016	10.6	9.1
16	5/11/2015	23.4	23.6	38	11/10/2016	8	6.4
17	21/12/2015	30	36.6	39	22/10/2016	12.2	12.7
18	6/01/2016	12.6	13.1	40	9/11/2016	25.2	13.7
19	15/01/2016	<i>20.3</i>	20.3	41	16/12/2016	24.8	20.5
20	21/01/2016	21.8	16.2	42	10/01/2017	11	12.3
21	29/01/2016	34.6	17.2				
22	4/02/2016	24.2	20.9				
23	8/05/2016	21.8	18.4				

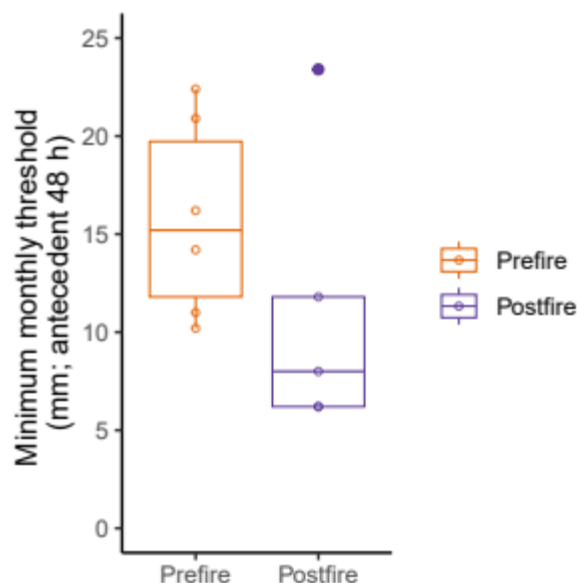
146

147 **Table 1.** Summary of recharge events. Data in italics: incomplete returns for the Bureau of Meteorology station on these dates. AWRA-L  
 148 data was used. Recharge event 7 occurred on 4<sup>th</sup> May 2015 and was a local rainfall event not captured in the gauge

149 The 48 h rainfall recharge thresholds for all events are presented in Table 1. Fig. 4 presents the rainfall recharge thresholds,  
 150 plotted by month and whether before or after the fire (Fig. 4a) and for all recharge events (Fig. 4b) using data from the Bureau  
 151 of Meteorology gauge. The median 48 h rainfall recharge threshold is 19.8 mm (mean: 26.2 mm). The lowest minimum 48 h



152 rainfall recharge threshold was 8.0 mm, observed after the fire in July and September, and the highest minimum was 25.2 mm,  
153 observed after the fire in November. Comparison between rain gauge and AWRA-L gridded daily precipitation yielded similar  
154 rainfall recharge thresholds (AWRA-L median: 17.2 mm; mean 22.0 mm).  
155



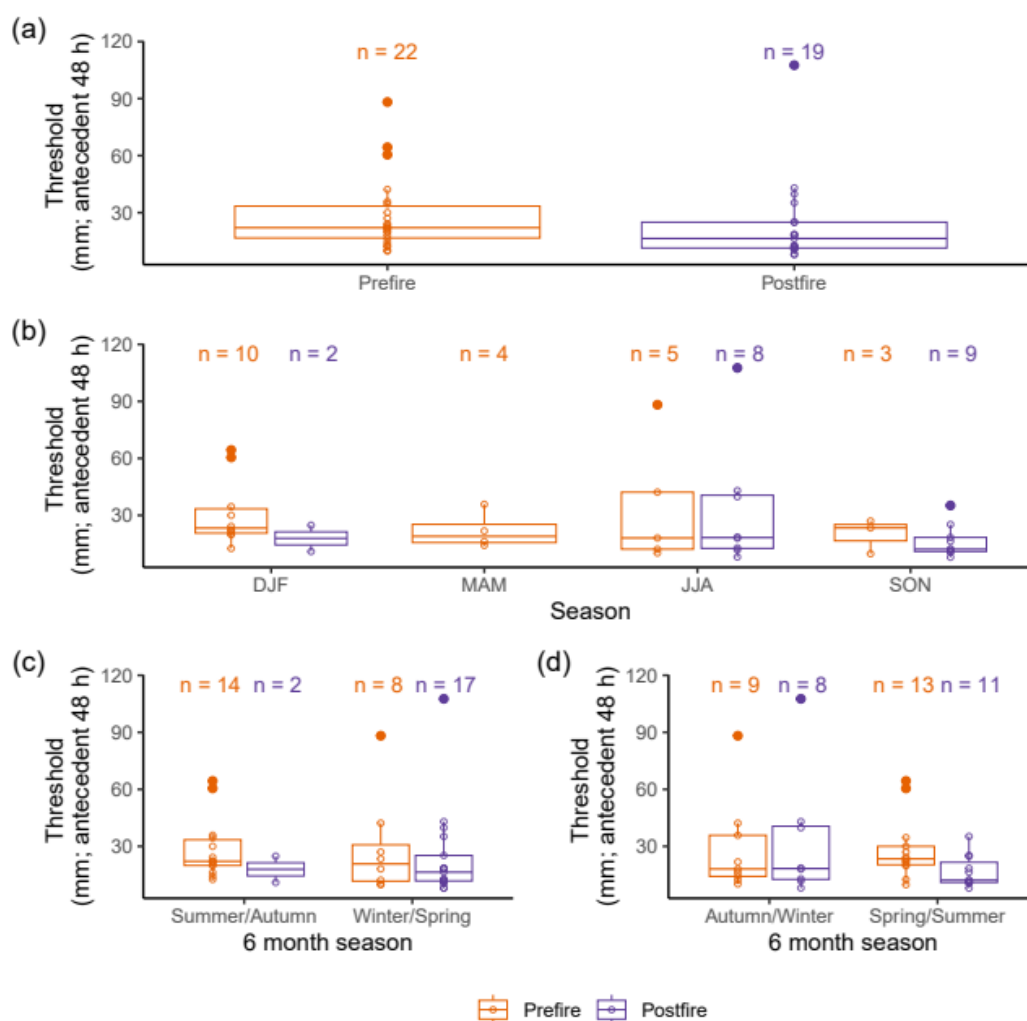
156 **Figure 6.** Minimum monthly rainfall recharge threshold (48 h, mm) for the pre fire (orange) and post fire (purple) periods  
157  
158 48 h rainfall recharge thresholds were compared before and after the fire. Because 48 h thresholds may be overestimated due  
159 to both the coarse sampling interval and the impact of extreme events, we first compared the minimum recharge threshold  
160 calculated for each month pre- and post-fire. Fig. 6 shows a qualitative reduction in the recharge threshold postfire using the  
161 minimum recharge in each month.

162  
163 We then analysed the 48 h rainfall recharge thresholds for all events before and after the fire using the Bureau of Meteorology  
164 station data. The median 48 h rainfall needed to generate recharge was 22.1 mm before the fire (n=22) and 16.4 mm after the  
165 fire (n=19) (Fig. 7a). The pre- and post-fire monitoring periods were of different lengths, with no reliable post-fire monitoring  
166 in the late summer / early autumn of 2017, when rainfall recharge thresholds might be expected to be higher due to enhanced  
167 evapotranspiration, and a Kruskal-Wallis ANOVA indicates these rainfall recharge thresholds are not significantly different at  
168 the 95% level.

169  
170 To overcome the different lengths of monitoring data before and after the fire, we undertook a stratified qualitative analysis  
171 by season. At this timescale, the number of recharge events in each season is too small for statistical analysis. However,  
172 considering December to February (DJF, summer), March to May (MAM, autumn), June to August (JJA, winter) and  
173 September to November (SON; spring)) there is qualitative evidence of a reduction in the post-fire recharge threshold in spring  
174 (SON) and summer (DJF) (Fig. 7b) (noting that there were 10 prefire events and 2 postfire events in DJF, and 3 prefire events



175 and 9 postfire events in SON). Aggregating these seasonal values into coarser categories (e.g. Summer/Autumn and  
 176 Winter/Spring, Fig. 7c; and Autumn/Winter and Spring/Summer, Fig. 7d) highlights a reduction in the postfire recharge  
 177 threshold relative to the prefire threshold in both the Spring/Summer (3-9 months post fire) and Summer/Autumn (6-12 months  
 178 post fire) categories, although the difference is more pronounced in the Spring/Summer data. This is likely owing to the absence  
 179 of post-fire MAM data due to the cessation of monitoring. While the Summer/Autumn and Winter/Spring categories are  
 180 unevenly sampled, the Autumn/Winter and Spring/Summer categories are evenly sampled. Trends in the seasonal data are  
 181 robust to the source of the precipitation information, identified in the thresholds calculated from both the BOM data (Fig.7)  
 182 and the AWRA-L data (Fig. A2).



183  
 184 **Figure 7.** Comparison of recharge thresholds pre-and post-fire using BOM data. Note that sample sizes are different depending on seasonal  
 185 grouping, most comparable for panel d, where Autumn/Winter have 9 samples for prefire, 8 samples for postfire, and spring/summer have 13  
 186 samples for prefire, 11 samples for postfire.



187 **4 Discussion**

188 The median rainfall recharge threshold at Wildman’s Cave (19.8 mm in 48 h) is comparable to two other temperate climate  
 189 sites using same methodology in south east Australia (Table 2). 41-67 mm/week of precipitation was needed before recharge  
 190 occurred at the South Glory Cave, Yarrangobilly, Australia (Baker et al., 2021). 76-79 mm/week of precipitation was needed  
 191 in caves in the Macleay region of New South Wales (Baker et al., (2020). The number of potential recharge events per year  
 192 (20 per year) observed at Wildman’s Cave is at the upper end of the range reported previously, with the most similar  
 193 characteristics at monitoring site LR1 at Yarrangobilly, which had the most recharge events per year for that site (17) and the  
 194 lowest rainfall recharge threshold (41 mm/week of precipitation) (Table 2).

Site	Climate (Köppen-Gieger)	Annual Precipitation (mm)	Lithology	Soil and vegetation	Number of events / year	Median 7-day rainfall recharge threshold (mm)	Median 48 h rainfall recharge threshold (mm)
Upper and Lower Macleay Caves, NSW 2014-2019	Cfa	1218	Permian limestone	Subtropical rainforest to dry subtropical rainforest	3.8 to 5.4	76 to 79	52 to 54 *
South Glory Cave, NSW 2013-2019	Cfb	1102	Silurian limestone	Red clays, thin loose soils and bare rock with sub-alpine open snow gum woodland	3.5 to 17	41 to 67	28 to 46 *
Wildman’s Cave, NSW 2014-2017	Cfb	802	Silurian marble	Bare to patchy soil, native shrubs and grasses	20		19.8

195  
 196 \*inferred assuming 69% of precipitation is within 48 h of the recharge event

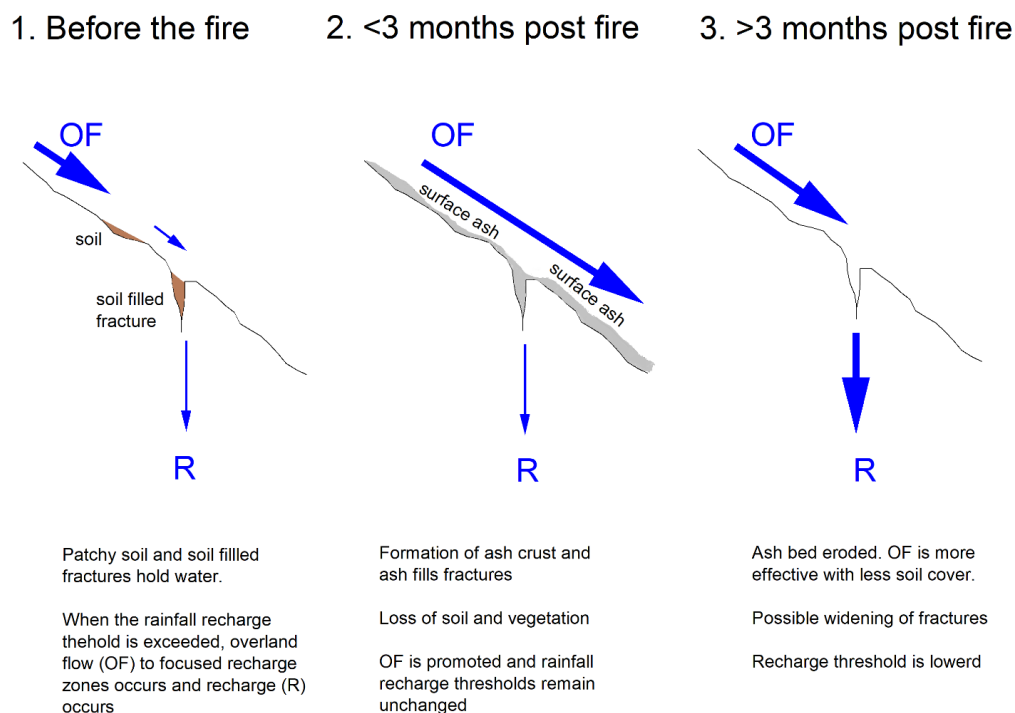
197 **Table 2.** Site info data from Baker et al. (2020, 2021) and this study. Cfa: temperate, no dry season, hot summer. Cfb: temperate, no dry  
 198 season, warm summer.

199  
 200 The effect of the intense fire on the rainfall recharge threshold is evident, with a decrease in the amount of rainfall needed. Our  
 201 results agree with changed hydrograph characteristics observed by Bian et al., (2019), interpreted as loss of diffuse flow  
 202 component, likely from loss or damage to soil and increased area of exposed bedrock, and local hotspots that damaged  
 203 limestone. We hypothesise that this loss of soil water storage would allow runoff generation to be more effective across areas  
 204 of bare limestone to the zones of focused recharge (Fig. 8). The decrease in rainfall recharge threshold is not observed  
 205 immediately post-fire, when the land surface above the cave was covered with thick ash deposits (see Fig. 1). Our observations  
 206 at the site showed a thick and widespread ash cover immediately post fire (Fig.1) which was absent four months post fire (Fig.  
 207 A3), with bare rock and absence of shrubby vegetation observed one year post-fire (Fig. A4). This is compatible with the



208 presence of ash produced by the high-severity experimental burn, combined with the moderate rainfall experienced in the days  
209 immediate post-fire (10.4 mm in the week following the experimental fire), resulting in the formation of an ash crust. This,  
210 combined with clogging of any remaining soil pores, retarded effective overland flow to the recharge zones (Woods and  
211 Balfour, 2008; Balfour et al., 2014; Bodí et al. 2014), reducing the number of recharge events in the months following the fire.  
212 When this ash was subsequently transported from the surface above the cave, the effect of soil removal and karst fracture  
213 enhancement, leading to enhanced infiltration, resulted in reduced rainfall recharge thresholds.

214



215 **Figure 8.** Conceptual figure of the recharge processes (1) before the fire (2) less than three months after the fire and (3) More than three months  
216 after the fire.

## 217 5 Conclusions

218 Our results from Wildman's Cave, with a median 48 h rainfall recharge threshold of 19.8 mm and 20 events per year, falls at  
219 the lower end of the range of previously observed rainfall recharge thresholds and higher end of the range for the number of  
220 potential recharge events per year across sites in temperate southern and eastern Australia, which have a median 48 h rainfall  
221 recharge greater than 28 mm and less than 17 events per year. Future studies should investigate these recharge characteristics  
222 across a diverse range of sites.

223



224 We provide direct measurements of the impact on fire on the potential for groundwater recharge, observing a delayed decrease  
225 in the rainfall recharge threshold occurring three months after a severe fire. The delayed change to the threshold is likely due  
226 to the presence of a thick ash bed, which likely prevented infiltration of precipitation. While we have demonstrated that a  
227 severe wildfire results in a lower recharge threshold, it is unknown whether a less-intense fire would have a similar effect.  
228 Similarly, this investigation was limited to three years of monitoring, and it is also not known whether this change in recharge  
229 threshold is permanent, or if the system will return to ‘pre-fire’ conditions following vegetation regrowth. Future work should  
230 aim to replicate this study with fires of different severities, and should include hydrological monitoring for some years after  
231 vegetation regrowth.

232

### 233 **Acknowledgements**

234

235 The research was partly funded by Australian Research Council Linkage LP13010017 and Laureate Fellowship FL240100057,  
236 and we acknowledge Andy Spate, Sophia Meehan and the Linkage project team for their contributions to overall project design.  
237 We thank Andrew Baker (National Parks and Wildlife Service) for site selection and Katie Coleborn for project management,  
238 and the team at Wombeyan Karst Conservation Reserve, especially manager David Smith. We would like to thank Fang Bian  
239 for helpful discussions when undertaking this data reanalysis.

240

### 241 **Competing interests**

242 The authors declare that they have no competing interests

243

### 244 **Data availability**

245 The hydrology data is available at [10.6084/m9.figshare.28169672](https://doi.org/10.6084/m9.figshare.28169672). All other hydroclimate datasets are publicly available from  
246 the Australian Bureau of Meteorology Climate Data Online (<http://www.bom.gov.au/climate/data/>) and Australian Water  
247 Outlook webpages (<https://awo.bom.gov.au/>). The karst area overlay used in Figure 1 is available at doi: [10.25928/b2.21\\_sfkq-  
248 r406](https://doi.org/10.25928/b2.21_sfkq-r406), the map concept is described in Chen et al., 2017. The Sentinel S2 visible image used in Figure 1 was retrieved from the  
249 Copernicus Dataspace (<https://dataspace.copernicus.eu/explore-data/data-collections/sentinel-data/sentinel-2>). The  
250 Wombeyan boundary is available from New South Wales government The Sharing and Enabling Environmental Data Portal  
251 [<https://datasets.seed.nsw.gov.au/dataset/9bad468a-c2a6-4c90-bfaa-8ae8af72e925>]. The digital elevation model is available  
252 from NSW Government, DFSI Spatial Services and accessed via Elvis - Elevation and Depth - Foundation Spatial Data  
253 (<https://elevation.fsdf.org.au/>).

254

### 255 **Author contributions**

256 CS performed initial data analysis and interpretation, MC provided additional data analysis and interpretation. AB undertook  
257 additional data analysis and wrote the first manuscript draft with contributions from all authors.



## 258 References

- 259 Ajami, H.: Geohydrology: Groundwater. Encyclopedia of Geology (Second Edition). D. Alderton and S. A. Elias. Oxford,  
260 Academic Press, 408-415, 2021.
- 261 Baker, A., Berthelin, R., Cuthbert, M.O., Treble, P.C., Hartmann, A. and the KSS Cave Studies Team: Rainfall recharge  
262 thresholds in a subtropical climate determined using a regional cave drip water monitoring network. *J. Hydrol.*, 587, 125001,  
263 2020
- 264 Baker, A., Scheller, M., Oriani, F., Mariethoz, G., Hartmann, A., Wang, Z. and Cuthbert, M.O.: Quantifying temporal  
265 variability and spatial heterogeneity in rainfall recharge thresholds in a montane karst environment. *J. Hydrol.*, 594, 125965,  
266 2021.
- 267 Baker, A., Shanafield, M., Timms, W., Andersen, M. S., Priestley, S., and Melo Zurita, M.: An underground drip water  
268 monitoring network to characterize rainfall recharge of groundwater at different geologies, environments, and climates across  
269 Australia, *Geosci. Instrum. Methods Data Syst.*, 13, 117-129, 2024
- 270 Balfour, V.N., Doerr, S.H., and Robichaud, P.R.: The temporal evolution of wildfire ash and implications for post-fire  
271 infiltration. *Int. J. Wildland Fire* 23, 733–745, doi:10.1071/WF13159, 2014.
- 272 Bian, F., Coleborn K., Flemons, I., Baker, A., Treble, P.C., Hughes, C.E., Baker, A., Andersen, M.S., Tozer, M.G., Duan, W.,  
273 Fogwill, C.J. and Fairchild, I.J.: Hydrological and geochemical responses of fire in a shallow cave system. *Sci. Total Environ.*,  
274 662, 180-191, 2019.
- 275 Boas, T and Mallants, D.: Episodic extreme rainfall events drive groundwater recharge in arid zone environments of central  
276 Australia. *J. Hydrology: Regional Studies*, 40, 101005, 2022.
- 277 Bodí, M.B., Martin, D.A., Balfour, V.N., Santín, C., Doerr, S.H., Pereira, P., Cerdà, A. and Mataix-Solera, J.: Wildland fire  
278 ash: Production, composition and eco-hydro-geomorphic effects. *Earth-Science Rev.*, 130, 103–127,  
279 doi:10.1016/j.earscirev.2013.12.007, 2014
- 280 Bureau of Meteorology: Australian Water Outlook, <https://awo.bom.gov.au/> access 9<sup>th</sup> December 2024
- 281 Cerdà, A.: Changes in overland flow and infiltration after a rangeland fire in a Mediterranean scrubland. *Hydrol. Proc.*, 12,  
282 1031–1042, doi: 10.1002/(SICI)1099-1085(19980615)12:7<1031::AID-HYP636>3.0.CO;2-V, 1998
- 283 Chen, Z., Goldscheider, N., Auler, A., Bakalowicz, M., Broda, S., Drew, D., Hartmann, J., Jiang, G., Moosdorf, N., Richts,  
284 A., Stevanovic, Z., Veni, G., Dumont, A., Aureli, A., Clos, P., and Krombholz, M.: World Karst Aquifer Map (WHYMAP  
285 WOKAM). BGR, IAH, KIT, UNESCO, doi: 10.25928/b2.21\_sfkq-r406, 2017
- 286 Frost, A. J., and Shokri, A.: The Australian Landscape Water Balance model (AWRA-L v7). Technical Description of the  
287 Australian Water Resources Assessment Landscape model version 7. Bureau of Meteorology Technical Report, 2021.
- 288 Gabet, E.J. and Sternberg, P.: The effects of vegetative ash on infiltration capacity, sediment transport, and the generation of  
289 progressively bulked debris flows. *Geomorphology*, 101, 666–673, doi: 10.1016/j.geomorph.2008.03.005, 2008.

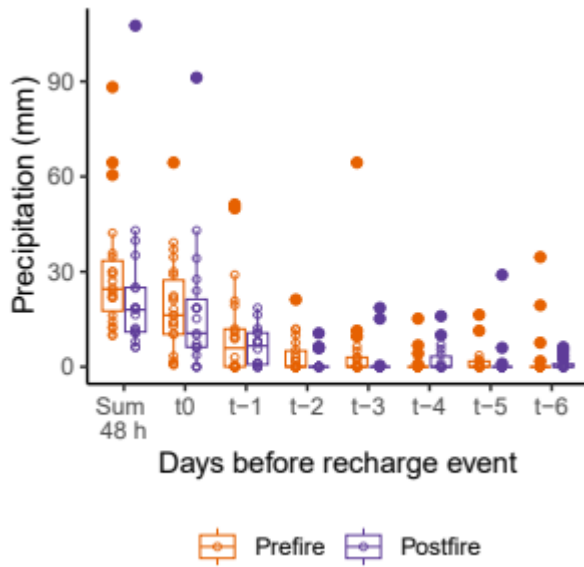


- 290 Healy, R.W. and Cook, P.G.: Using groundwater levels to estimate recharge. *Hydrogeol. J.*, 10, 91–109, doi: 10.1007/s10040-  
291 001-0178-0, 2002.
- 292 Kotchoni, D.O.V., Vouillamoze, J.M., Lawson, F.M.A., Adjomayi, P., Boukari, M. and Taylor, R.G.: Relationships between  
293 rainfall and groundwater recharge in seasonally humid Benin: a comparative analysis of long-term hydrographs in sedimentary  
294 and crystalline aquifers. *Hydrogeol. J.*, 27, 447–457, doi: 10.1007/s10040-018-1806-2, 2019.
- 295 Osborne, R.A.: The History of Karstification at Wombeyan Caves, New South Wales, Australia, as revealed by Palaeokarst  
296 Deposits, *Cave Science*, 20, 1-8, 1993
- 297 Noori, R., Maghrebi, M., Jessen, S., Bateni, S.M., Heggy, E., Javadi, S., Noury, M., Pistre, S., Abolfathi, S., and AghaKouchak,  
298 A.: Decline in Iran’s groundwater recharge. *Nat. Commun.*, 14, 6674, doi: 10.1038/s41467-023-42411-2, 2023
- 299 Onda, Y., Dietrich, W.E. and Booker, F.: Evolution of overland flow after a severe forest fire, Point Reyes, California. *Catena*,  
300 72, 13–20, doi: 10.1016/j.catena.2007.02.003, 2008.
- 301 Pepler, A., Coutts-Smith, A. and Timbral, B.: The role of East Coast Lows on rainfall patterns and inter-annual variability  
302 across the East Coast of Australia. *Int. J. Climatol.* 34 1011-2021, doi: 10.1002/joc.3741, 2014
- 303 Rohde, M.M., Albano, C.M., Huggins, X., Klausmeyer, K.R., Morton, C., Sharman, A., Zaveri, E., Saito, L., Freed, Z.,  
304 Howard, J.K., Job, N., Richter, H., Toderich, K., Rodella, A.-S., Gleeson, T., Huntington, J., Chandanpurkar, H.A., Purdy,  
305 A.J., Famiglietti, J.S., Singer, M.B., Roberts, D.A., Caylor, K. and Stella, J.C.: Groundwater-dependent ecosystem map  
306 exposes global dryland protection needs. *Nature*, 632, 101–107, doi: 10.1038/s41586-024-07702-8, 2024.
- 307 Woods, S.W. and Balfour, V.N.: The effect of ash on runoff and erosion after a severe forest wildfire, Montana, USA. *Int. J.*  
308 *Wildland Fire* 17, 535–548, doi: 10.1071/WF07040, 2008.
- 309 Wylie J. and Wylie G.: The caves of Wombeyan: An annotated listing. In: *Caves and Karst of Wombeyan*. Sydney  
310 *Speleological Society Occasional Paper*, 13, 167-196, 2004.
- 311



312 **Appendix**

313



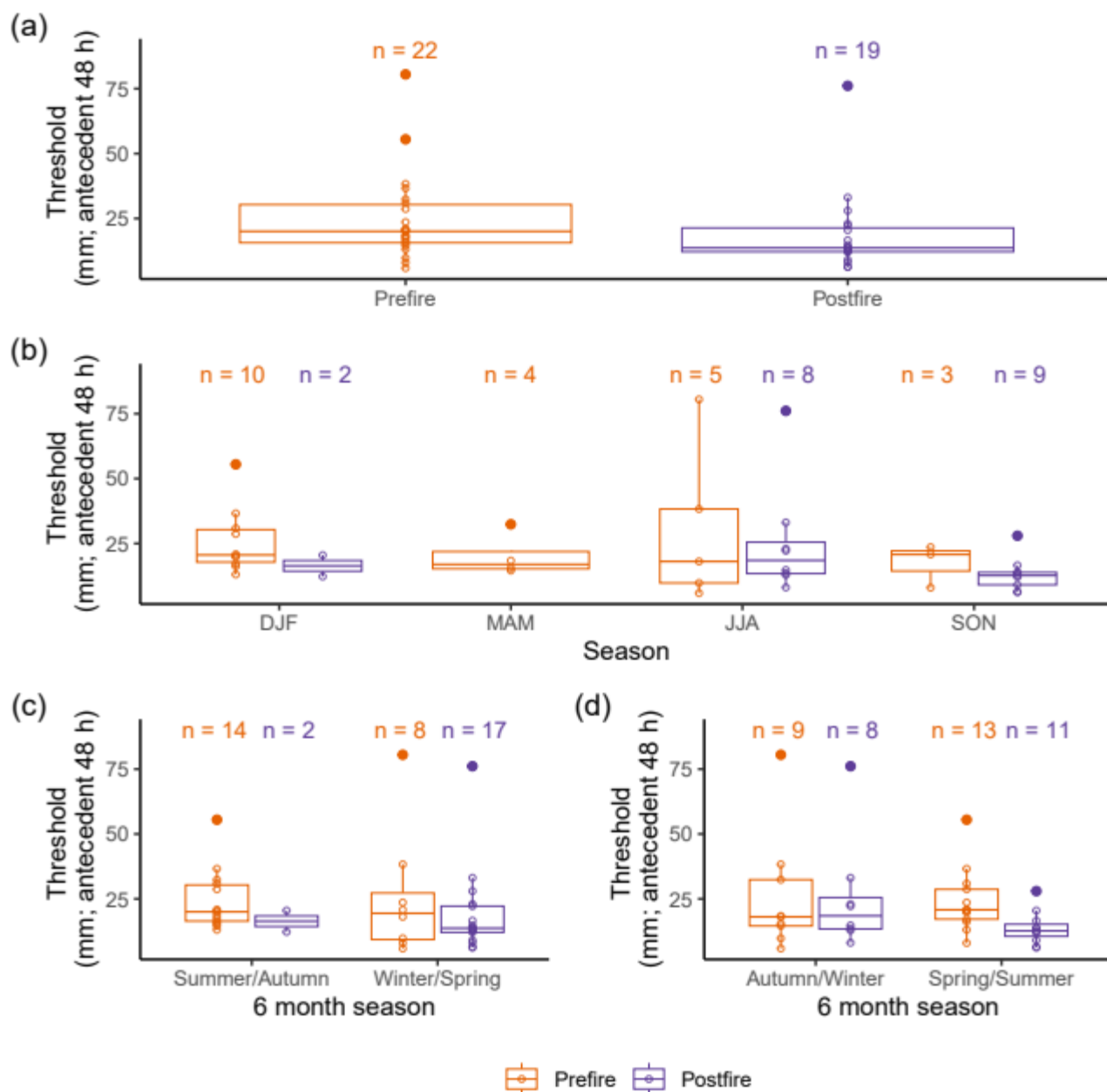
314

315 **Figure A1.** The amount of precipitation summed over the 48 hours prior to recharge compared to the amount of rainfall in each of the seven  
316 days prior to recharge. Precipitation data is shown for recharge events pre-fire (orange) and post-fire (purple).

317



318



319

320 **Figure A2.** Comparison of recharge thresholds pre-and post-fire using AWRA-L data. Note that sample sizes are different depending on  
 321 seasonal grouping, most comparable for panel d, where Autumn/Winter have 9 samples for prefire, 8 samples for postfire, and spring/summer  
 322 have 13 samples for prefire, 11 samples for postfire.  
 323

324

325



325



326

327 **Figure A3.** Four months post fire. Note the lack of surface ash. View is across slope, cave entrance is in foreground. Photo credit: Andy  
328 Baker

329



343 **Figure A4** One year post fire. Note lack of shrubby vegetation and patches of exposed limestone. View is downslope, Wildman's Cave is  
344 beneath the foreground surface. Photo credit: Andy Baker

345